

P O L S K A      A K A D E M I A      N A U K

I N S T Y T U T   M A S Z Y N   P R Z E P Ł Y W O W Y C H

**TRANSACTIONS  
OF THE INSTITUTE OF  
FLUID-FLOW MACHINERY**

**PRACE**

**I N S T Y T U T U   M A S Z Y N   P R Z E P Ł Y W O W Y C H**

**107**

Selected papers from the First Polish-Japanese  
Hakone Group Symposium on Nonthermal Plasma  
Processing of Water and Air, Sopot, Poland,  
May 29-31, 2000



GDAŃSK 2000

THE TRANSACTIONS OF THE INSTITUTE OF FLUID-FLOW MACHINERY

---

exist for the publication of theoretical and experimental investigations of all aspects of the mechanics and thermodynamics of fluid-flow with special reference to fluid-flow machines

\*

PRACE INSTYTUTU MASZYN PRZEPLYWOWYCH

---

poświęcone są publikacjom naukowym z zakresu teorii i badań doświadczalnych w dziedzinie mechaniki i termodynamiki przepływów, ze szczególnym uwzględnieniem problematyki maszyn przepływowych

*Wydanie publikacji zostało dofinansowane przez PAN ze środków DOT uzyskanych z Komitetu Badań Naukowych*


EDITORIAL BOARD – RADA REDAKCYJNA

ZBIGNIEW BILICKI \* BRUNON GROCHAL \* JAN KICIŃSKI  
JAROSŁAW MIKIELEWICZ (CHAIRMAN – PRZEWODNICZĄCY)  
JERZY MIZERACZYK \* WIESŁAW OSTACHOWICZ  
WOJCIECH PIETRASZKIEWICZ \* ZENON ZAKRZEWSKI

EDITORIAL COMMITTEE – KOMITET REDAKCYJNY

JAROSŁAW MIKIELEWICZ (EDITOR-IN-CHIEF – REDAKTOR NACZELNY)  
ZBIGNIEW BILICKI \* JAN KICIŃSKI  
EDWARD ŚLIWICKI (EXECUTIVE EDITOR – REDAKTOR)

EDITORIAL OFFICE – REDAKCJA

Wydawnictwo Instytutu Maszyn Przepływowych  
Polskiej Akademii Nauk  
ul. Gen. Józefa Fiszera 14, 80-952 Gdańsk, skr. poczt. 621,  
 (0-58) 341-12-71 wew. 141, fax: (0-58) 341-61-44,  
e-mail: esli@imp.gda.pl

ISSN 0079-3205

SEIJI KANAZAWA, DUAN LI, SHUICHI AKAMINE, TOSHIKAZU OHKUBO,  
YUKI HARU NOMOTO<sup>1</sup>

## Decomposition of toluene by a dielectric barrier discharge reactor with a catalyst coating electrode

The improvement in the decomposition of volatile organic compounds (VOCs) was investigated by combining discharge plasma with photocatalyst ( $\text{TiO}_2$ ). The reactor consists of a coaxial cylindrical electrode system and dielectric barrier discharge is used for the processing. In order to combine discharge plasma with photocatalyst, an electrode with photocatalyst was developed as an inner electrode instead of the conventional metal electrode. Time dependence of toluene decomposition was compared for the reactors with and without photocatalyst. As a result, in dilute toluene (20-25 ppm) at an energy consumption of 18 J/l, time averaged toluene decomposition rates by the conventional type reactor, the photocatalyst-plasma reactor with  $\text{TiO}_2$  pellets, the photocatalyst-plasma reactor with  $\text{TiO}_2$  coating electrode were 31% at 5.8 g/kWh energy efficiency, 45% at 6.9 g/kWh, and 59% at 8.9 g/kWh, respectively. It was found that the combination of the plasma and  $\text{TiO}_2$  was effective for improving toluene decomposition at lower applied voltages and the lower energy consumption.

### 1. Introduction

Emission of various volatile organic compounds (VOCs) from the semiconductor and paint industries is one of the causes of air pollution. Nonthermal plasma processing has been considered as the effective method to remove VOCs. The plasma processings for removing VOCs include electron beam [1], surface discharge [2], dielectric barrier discharge [3, 4], ferroelectric packed-bed [5, 6], pulsed corona [1], [5], DC discharge [7, 8] and microwave discharge processes [9]. However, the issues to be solved are the improvement of the energy efficiency and the control of undesirable by-products.

To improve the energy efficiency, utilization of catalyst/adsorbent into plasma has been investigated [10-15]. In this process, if a catalyst can be activated using the plasma, the energy efficiency may be improved due to synergetic effects

<sup>1</sup>Dept. of Electrical and Electronic Engineering, Oita University, 700 Dannoharu, Oita 870-1192, Japan

of catalytic reactions and plasma induced chemical reactions. To activate a catalyst/adsorbent and avoid the generation of undesirable by-products, the control of plasma state is very important.

In this study, the effect of the combination of plasma with photocatalyst ( $\text{TiO}_2$ ) on the decomposition of VOCs has been investigated experimentally. The key idea is to use a photocatalyst-coating electrode for a barrier discharge reactor instead of the conventional metal electrode. Toluene ( $\text{C}_6\text{H}_5\text{CH}_3$ ) was chosen due to a typical VOCs as well as a fact that it exists not only in paint industry but also in houses. This paper describes the decomposition of dilute toluene using three types of dielectric barrier discharge plasma reactors.

## 2. Experimental apparatus

The decomposition of toluene was investigated using three types of reactors shown in Fig. 1, i.e. (1) a conventional dielectric barrier discharge reactor (a photocatalyst-free-plasma reactor), (2) a photocatalyst-plasma reactor with  $\text{TiO}_2$  pellets, and (3) a photocatalyst-plasma reactor with  $\text{TiO}_2$  coating electrode.

The basic configuration of these reactors is the same except for the inner electrodes. The reactor consists of a quartz glass tube of 21 mm inner diameter with 1.5 mm thickness and 300 mm length. The stainless-steel mesh wrapped on the quartz glass tube was used as an outer electrode. The diameter of the cylindrical inner electrode is 18.5 mm. The gap distance for discharges is 1.25 mm.

In Fig. 1(b), the inner electrode consists of coaxial placed stainless-steel rings (o.d. 18.5 mm, width 10 mm, thickness 2 mm) with  $\text{TiO}_2$  pellets. A commercially available photocatalyst, pellet of  $\text{TiO}_2$  with 2 mm in average diameter and a specific surface area of  $250 \text{ m}^2/\text{g}$  (Ishihara Techno Co. Ltd., ST-A31,  $\text{TiO}_2$  content 81 wt.%), was utilized. The  $\text{TiO}_2$  pellets were packed into the grooves formed by the metal rings as shown in Fig. 1(b). About 17% of inner electrode surface consist of  $\text{TiO}_2$  pellets. While, in Fig. 1(c), the whole surface of inner electrode was coated by the paint containing  $\text{TiO}_2$ . This photocatalyst coating was conducted by a paint with a brush coating method using a commercially available photocatalyst paint (Okitsumo Co. Ltd., ecoatio<sub>2</sub>).

The paint consists of fine  $\text{TiO}_2$  powder and silicon based resin. Surface/cross-sectional structure of the coating was examined by scanning electron microscopy (SEM). The thickness of the coating layer was ca 20-30  $\mu\text{m}$ .

The experimental flow loop used in this study is shown schematically in Fig. 2. As a test gas, air containing toluene was introduced to the reactor. Toluene concentration was measured by a gas chromatograph (Shimazu, GC-8A). The gas flow rate was 0.5-1 l/min.

The discharge was triggered after the toluene concentration reached a steady state. AC high voltage (60 Hz) was applied between the inner and outer electrodes and dielectric barrier discharge was generated. The discharge power was measured by the Lissajous figure method [16]. The experiment was carried out at room temperature and under atmospheric pressure.

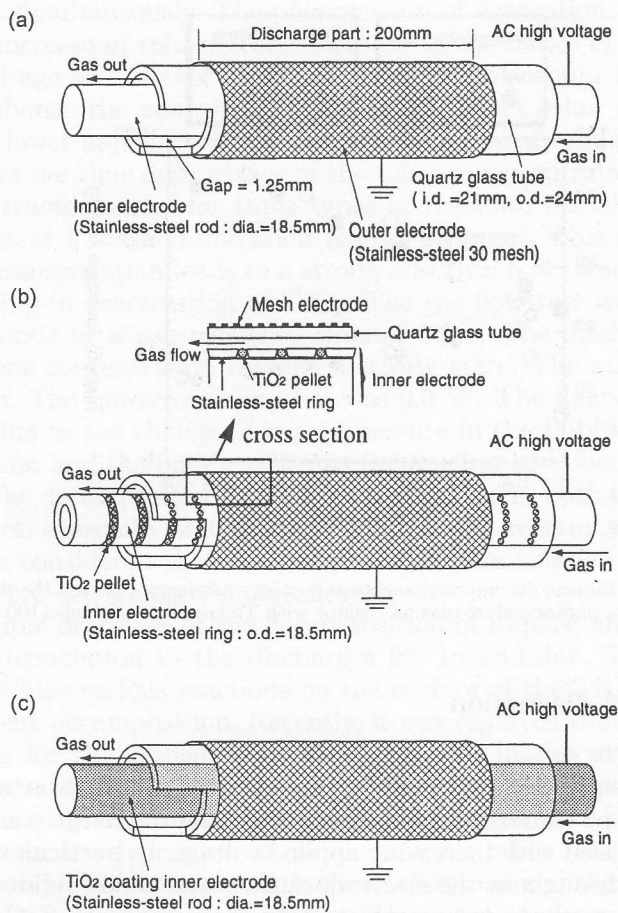


Fig. 1. Schematic diagram of three types of reactors: (a) dielectric barrier discharge reactor, (b) photocatalyst-plasma reactor with TiO<sub>2</sub> pellets, (c) photocatalyst-plasma reactor with TiO<sub>2</sub> coating electrode.

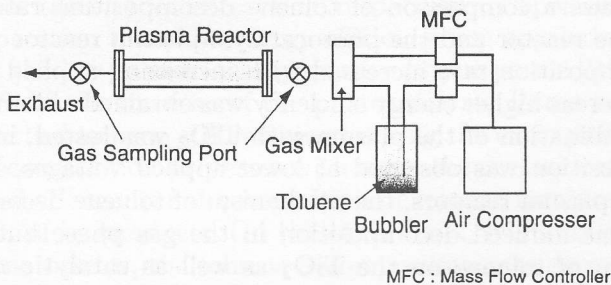


Fig. 2. Schematic diagram of experimental flow loop.



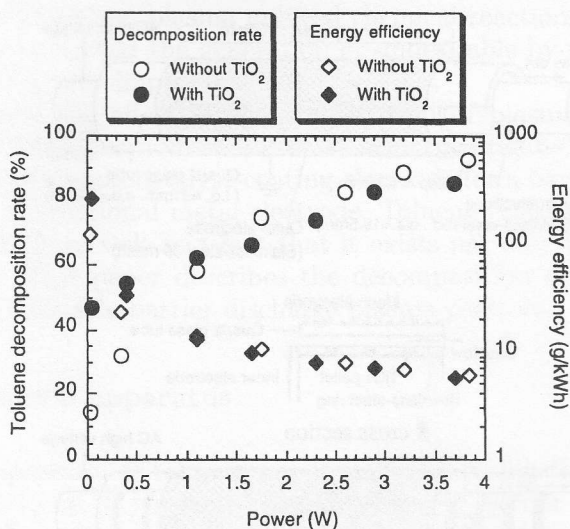


Fig. 3. Comparison of toluene decomposition rate and energy efficiency between the dielectric barrier discharge reactor and the photocatalyst-plasma reactor with TiO<sub>2</sub> pellets. Toluene(100 ppm)/Air:1 l/min.

### 3. Results and discussion

With the present reactors, the dielectric barrier discharge starts at the applied voltage of 7 kVp-p. Uniform luminescence from the discharge was observed and its intensity increased with increasing applied voltage. In particular, the discharge glows uniformly throughout the electrode surface and is not divided into separate filaments for the case of photocatalyst-plasma reactor with TiO<sub>2</sub> coating electrode. This is due to the presence of semiconducting TiO<sub>2</sub> coating layer onto the inner electrode. It was reported that the distributed resistance of a semiconducting electrode affected the discharge mode [17]. Discharge power calculated from the Lissajous figure was between 0.1 to 4 W depending on the applied voltage.

Fig. 3 shows a comparison of toluene decomposition rate between the conventional type reactor and the photocatalyst-plasma reactor with TiO<sub>2</sub> pellets. Toluene decomposition rate increased with increasing applied voltage or the input power, whereas higher energy efficiency was obtained at lower applied voltage. When the combination of the plasma with TiO<sub>2</sub> was tested, improvement of toluene decomposition was observed at lower applied voltages. In the case of the photocatalyst-plasma reactors, the mechanism of toluene decomposition involves not only plasma-induced decomposition in the gas phase but also the adsorption/desorption of toluene on the TiO<sub>2</sub> as well as catalytic reaction. At lower applied voltages or lower input powers, plasma decomposition is relatively weak and adsorption is dominant at the initial stages. While, at higher applied voltages or higher input powers, plasma decomposition is strong and desorption due to the

plasma occurs simultaneously. The phenomenon of desorption was confirmed by the temporal increase of toluene concentration at the outlet of the reactor when the applied voltage was further increased. Taking into account these phenomena, in order to enhance the advantage of synergistic effect other experiments were carried out at lower applied voltages and the lower energy consumption.

Fig. 4 shows the time dependence of the toluene concentrations at the reactor inlet and the reactor outlet for three types of reactors. Initial concentration of toluene was set at lower concentration (ca. 20-25 ppm). This is due to the fact that a higher concentration leads to a strong adsorption of toluene onto the  $\text{TiO}_2$  surface, resulting in deactivation of  $\text{TiO}_2$ . The gas flow rate was set at 1 l/min, which corresponds to a gas residence time of 0.9 s. The discharge was started after the toluene concentration reached a steady state. The applied voltage was set at 9 kVp-p. The power consumption was 0.3 W. The fluctuation of the concentration is due to the change of vapor pressure in the bubbler. The difference between the inlet and the outlet indicates the amount of toluene decomposed. It is found that the decomposition of toluene is enhanced in both the photocatalyst-plasma reactors, especially the photocatalyst-plasma reactor with  $\text{TiO}_2$  coating electrode. It is considered that the gas phase toluene and the toluene adsorbed on the  $\text{TiO}_2$  were decomposed simultaneously.

The principle processes of the decomposition of toluene are electron and radical impact dissociation in the discharges [8]. In addition,  $\text{TiO}_2$  activated by plasma may induce various reactions on the surface of the  $\text{TiO}_2$ , resulting in an enhanced toluene decomposition. Recently, it was reported that ozone played the important role for the activation of  $\text{TiO}_2$  [18, 19]. In this study, we have not measured the gas phase by-products except for  $\text{CO}_2$ . The formation of  $\text{CO}$ ,  $\text{CO}_2$ ,  $\text{O}_3$ ,  $\text{NO}$ ,  $\text{N}_2\text{O}$ , and  $\text{HNO}_3$  was reported as typical by-products [4], [8, 9]. After the experimental run, the deposition of carbon or some other reaction products was also identified on both the surface of the inner electrode and the wall of the quartz glass tube as the solid-phase by-products. It has been confirmed that this tar-like substance could be removed by the plasma in fresh air flow [20]. Moreover, the co-injection of ozone or hydrogen peroxide into the reactor has been considered to be effective in the decomposition performance [18].

Fig. 5 shows the time dependence of the toluene decomposition rate and the energy efficiency for three types of reactors, respectively. Depending on the types of reactors and operation time, the energy efficiency was approximately between 2 to 14 g/kWh at the low specific energy density (input power [W]/gas flow rate [l/s] = [J/l]) of 18 J/l. In the case of the photocatalyst-plasma reactors, the influence of the adsorbed toluene still remained during the early period. Due to the desorption and decomposition processes with time, the surface condition may be gradually recovered. Hence, the decomposition of toluene increased with time in spite of generation of by-products. On the other hand, in the case of the photocatalyst free-plasma reactor, the toluene decomposition rate decreased with time due to the deposition of by-products onto both the surface of the inner electrode and the wall of the reactor. Therefore, the decomposition rate was improved by using the photocatalyst-plasma reactors.

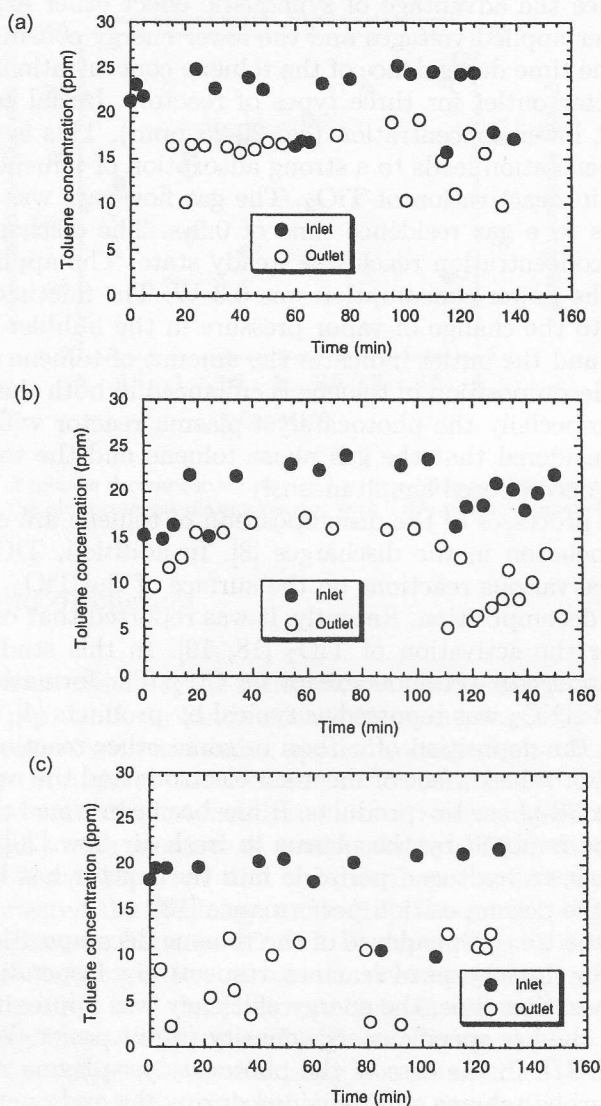


Fig. 4. Time dependence of toluene concentration at the inlet and outlet for there types of reactors: (a) dielectric barrier discharge reactor, (b) photocatalyst-plasma reactor with  $\text{TiO}_2$  pellets, (c) photocatalyst-plasma reactor with  $\text{TiO}_2$  coating electrode.



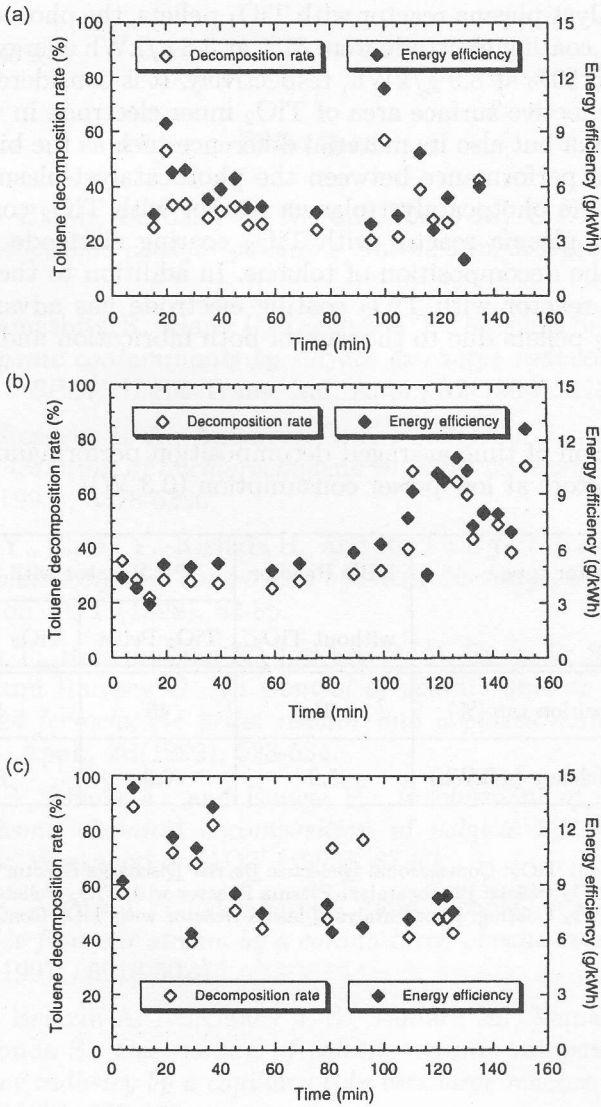


Fig. 5. Time dependence of toluene decomposition rate and energy efficiency: (a) dielectric barrier discharge reactor, (b) photocatalyst-plasma reactor with TiO<sub>2</sub> pellets, (c) photocatalyst-plasma reactor with TiO<sub>2</sub> coating electrode.

Based on the data presented in Fig. 5, Table 1 summaries comparison of the decomposition performance for three types of reactors. At an energy consumption of 18 J/l, time averaged toluene decomposition rates by the conventional type reactor, the photocatalyst-plasma reactor with  $\text{TiO}_1$  pellets, the photocatalyst-plasma reactor with  $\text{TiO}_2$  coating electrode were 31% at 5.8 g/kWh energy efficiency, 45% at 6.9 g/kWh, and 59% at 8.9 g/kWh, respectively. It is considered that not only the difference in effective surface area of  $\text{TiO}_2$  inner electrode in which is in contact with the plasma but also its material difference such as the binder may affect the decomposition performance between the photocatalyst-plasma reactor with  $\text{TiO}_2$  pellets and the photocatalyst-plasma reactor with  $\text{TiO}_2$  coating electrode. The photocatalyst-plasma reactor with  $\text{TiO}_2$  coating electrode shows the best performance for the decomposition of toluene. In addition to the decomposition performance, the reactor with  $\text{TiO}_2$  coating electrode has advantages over the reactor with  $\text{TiO}_2$  pellets due to the ease of both fabrication and maintenance.

Table 1. Comparison of time averaged decomposition performance of toluene for three types of reactors at low power consumption (0.3 W)

Reactor type	DBD Reactor	PP Reactor with $\text{TiO}_2$	
	without $\text{TiO}_2$	$\text{TiO}_2$ Pellet	$\text{TiO}_2$ Coating
Decomposition rate(%)	31	45	59
Energy efficiency (g/kWh)	5.8	6.9	8.9

Legend:

DBD Reactor without  $\text{TiO}_2$ : Conventional Dielectric Barrier Discharge Reactor

PP Reactor with  $\text{TiO}_2$  Pellets: Photocatalyst-Plasma Reactor with  $\text{TiO}_2$  Pellets

PP Reactor with  $\text{TiO}_2$  Coating: Photocatalyst-Plasma Reactor with  $\text{TiO}_2$  Coating Electrode

#### 4. Conclusion

The photocatalyst-plasma processing system for VOC treatment was developed and the decomposition of toluene was investigated experimentally. We used a photocatalyst-coating electrode for a barrier discharge plasma reactor instead of the conventional metal electrode. This coating electrode plays an important role not only in the discharge properties but also in the treatment of toluene in air. It was found that the combination of the plasma and  $\text{TiO}_2$  was effective for improving toluene decomposition at lower applied voltages and lower concentration.

**Acknowledgements** This work was supported in part by a Grant-in-Aid for Scientific Research from the Ministry of Education, Science, Sports and Culture of Japan.

Received 15 August 2000

### References

- [1] Penetrante B. M., Bardsley J. N., and Hsiao M. C.: *Kinetic analysis of non-thermal plasma used for pollution control*, Jpn. J. Appl. Phys., **36**(1997), 5007-5017.
- [2] Oda T., Yamashita R., Haga I., Takahashi T., Masuda S: *Decomposition of gaseous organic contaminants by surface discharge induced plasma chemical processing - SPCP*, IEEE Trans. Ind. Appl., **32**(1996), 118-123.
- [3] Evans D., Rosocha L. A., Anderson G. K., Coogan J. J., and Kushner M. J.: *Plasma remediation of trichloroethylene in silent discharge plasmas*, J. Appl. Phys., **74**(1993), 5378-5386.
- [4] Miyagawa Y., Ehara Y., Kishida H., and Ito T.: *Effect of oxygen on decomposition of volatile organic compounds by silent discharge*, Proc. of Asia-Pacific Workshop on AOT (1998), 83-86.
- [5] Yamamoto T., Ramanathan K., Lawless P. A., Ensor D. S., Newsome J. R., Plaks N., and Ramsey G. H.: *Control of volatile organic compounds by an ac energized ferroelectric pellet reactor and a pulsed corona reactor*, IEEE Trans. Ind. Appl., **28**(1992), 528-534.
- [6] Futamura S., Zhang A., and Einaga H.: *Involvement of active oxygen species in plasma chemical decomposition of volatile hydrocarbons*, Proc. of Asia-Pacific Workshop on AOT (1998), 87-90.
- [7] Chang J. S., Myint T., Chakrabarti A., and Miziolek A.: *Removal of carbon tetrachloride from air stream by a corona torch plasma reactor*, Jpn. J. Appl. Phys., **36**(1997), 5018-5024.
- [8] Kohno H., Berezin A. A., Chang J. S., Tamaru M., Yamamoto T., Shibuya A., and Honda S.: *Destruction of volatile organic compounds used in a semiconductor industry by a capillary tube discharge reactor*, IEEE Trans. Ind. Appl., **34**(1998), 953-966.
- [9] Mizeraczyk J.: *Microwave torch plasma at atmospheric pressure for decomposition of hydrocarbons*, Papers of Tech. Meeting on Electrical Discharges, ED-99-88, IEE Japan (1999), 63-66.
- [10] Yamamoto T., Mizuno K., Tamori I., Ogata A., Nifuku M., Michalska M., and Prieto G.: *Catalysis-assisted plasma technology for carbon tetrachloride destruction*, IEEE Trans. Ind. Appl., **32**(1996), 100-105.

- [11] Oda T., Kato T., Takahashi T., and Shimizu K.: *Nitric oxide decomposition in air by using non-thermal plasma processing with additives and catalyst*, IEEE Trans. Ind. Appl., **34**(1998), 268-272.
- [12] Mizuno A., Kisanuki Y., Noguchi M., Katsura S., Lee S. H., Hong Y. K., Shin S. Y, and Kang J. H.: *Indoor air cleaning using a pulsed discharge plasma*, IEEE Trans. Ind. Appl., **35**(1999), 1284-1288.
- [13] Ogata A., Yamanouchi K., Mizuno K., Kushiyama S., and Yamamoto T.: *Decomposition of benzene using alumina-hybrid and catalyst-hybrid plasma reactor*, IEEE Trans. Ind. Appl., **35**(1999), 1289-1295.
- [14] Kim H. H, Tsunoda K., Katsura S., Mizuno A.: *A novel plasma reactor for NO<sub>x</sub> control using photocatalyst and hydrogen peroxide injection*, IEEE Trans. Ind. Appl., **35**(1999), 1306-1310.
- [15] Shimizu K., and Oda T.: *DeNO<sub>x</sub> process in flue gas combined with nonthermal plasma and catalyst*, IEEE Trans. Ind. Appl., **35**(1999), 1311-1317.
- [16] Chang J. S., Kelly A. J., and Crowley J. M. ed.: *Handbook of Electrostatic Processes* Marcel Dekker, Inc., (1995), 586-588.
- [17] Salamov B. G., Ellialtioglu S., Akinoglu B. G., Lebedeva N. N., and Patriskii L. G.: *Spatial stabilization of townsend and glow discharges with a semiconducting cathode*, J. Phys. D: Appl. Phys., **29**(1996), 628-633.
- [18] Alberici R. M., and Jardim W. F.: *Gas phase destruction of VOCs using TiO<sub>2</sub>/UV and TiO<sub>2</sub>/O<sub>3</sub>/UV*, J. Adv. Oxid. Technol., **3**(1998), 182-187.
- [19] Kisanuki Y., Yoshida M., Takashima K., Katsura S., Mizuno A., Lee S. H., Hong Y. K., Kang K. O.: *Study on indoor air cleaning using plasma reactor combined with catalyst*, J. Inst. Electrostat. Jpn., **24**(2000) 153-158.
- [20] Yamaguma S., Ohsawa A., Kodama T., and Tabata Y.: *Decomposition of volatile organic compounds by plasma chemical process*, Proc. of 1992 Annual Meeting of the Inst. Electrostat. Jpn. (1992), 103-106.

## Rozkład toluenu w reaktorze wyładowania dielektrycznego z elektrodą pokrytą katalizatorem

### Streszczenie

Badano możliwość zwiększenia skuteczności rozkładu lotnych związków organicznych w powietrzu poprzez jednoczesne zastosowanie plazmy wyładowania elektrycznego i katalizatora (TiO<sub>2</sub>). Reaktor wyładowania dielektrycznego zbudowany był z układu współosiowych elektrod cylindrycznych. Elektroda wewnętrzna pokryta była katalizatorem. Porównano rozkład toluenu w czasie dla reaktora z katalizatorem i bez katalizatora. Wyniki badań wykazały, że w mieszaninie powietrza z toluenem (20-25 ppm), przy zużyciu energii 18 J/dm<sup>3</sup>, skuteczność rozkładu toluenu wynosiła: w reaktorze bez katalizatora – 31%, przy wydajności 5,8 g/kWh; w reaktorze z pastylkami TiO<sub>2</sub> – 45%, przy wydajności 6,9 g/kWh; w reaktorze z elektrodą wewnętrzną pokrytą TiO<sub>2</sub> – 59%, przy wydajności 8,9 g/kWh. Z przeprowadzonych badań wynika, że zastosowanie kombinacji wyładowania dielektrycznego z katalizatorem zwiększa skuteczność rozkładu toluenu w powietrzu przy niskich napięciach zasilania i małym zużyciu energii.



2<sup>nd</sup> plasma desorption took place at  $V_p = 10$  kV for 30 min. This process was repeated three times to characterize the plasma desorption and regeneration for MS-13X which was shown in Fig. 5. It is clear that the quantity of NO desorption increases with the repeating adsorption. The amount of NO desorption can be estimated by the ratio of the area of the desorption curve to the total adsorption. The amount of NO desorption by the first plasma desorption was approximately 7.5% of the total NO adsorbed.

The second desorption was 13% if first adsorption was taken into account or 20% when only second adsorption was considered. The third adsorption was 15%, if three adsorptions were considered or 38% when only third adsorption was considered. Speculation for the superior desorption characteristics for the repeated adsorption is as follows: freshly adsorbed NO laid on top of previously adsorbed NO, which results in previously adsorbed NO, penetrates further towards the central pores of MS-13X pellets. The NO after third adsorption was accumulated near the surface. Therefore, when the plasma was applied, NO can be easily desorbed into the gas stream [5].

The desorption rate can be expressed as the product of concentration and flow rate. The desorption rate after 2<sup>nd</sup> adsorption and desorption process was plotted in Fig. 6. The highest desorption rate was achieved when the flow rate was 5 l/min for the first 5 min but tailed down as time elapsed. It is also clear that the highest quantity of NO was desorbed with 1.2 l/min flow rate if it was expressed for 30 min. These results suggest that the short period of plasma desorption with high flow rate (intermittent desorption) is most preferable operation to achieve the maximum desorption for the case of NO.

### 3.4. Adsorption/desorption characteristics for low $\text{NO}_x$ concentration

In the previous study, we used 1,000~4,000 ppm  $\text{NO}_x$  to accelerate the experiments. We needed to confirm the adsorption and desorption characteristics for low  $\text{NO}_x$  concentration (measured as  $\text{NO}_x$ ) which is more realistic for industrial applications. Fig. 7(a) shows the adsorption characteristics for 100 ppm  $\text{NO}_x$ . The  $\text{NO}_x$  was maintained at 15 ppm after 10 h of operation when the flow rate was at 1.0 l/min. Adsorbed NO was desorbed using the 20 kHz AC power supply ( $V_p = 5$  kV). The 100 ppm  $\text{NO}_x$  was condensed to 2,500 ppm after 3 min with the flow rate of 1.2 l/min as shown in Fig. 7(b). The desorption characteristics was comparable to Fig. 3 and superior compared with the 60 Hz AC power supply although the difference of adsorption distribution was not clear at the present stage.

When the 20 kHz power supply was used, the desorption may be attributed to both plasma and temperature. The  $\text{NO}_x$  and CO concentrations were measured when the plasma was applied to MS-13X in air. The reactor surface temperature reached 170°C and thus the gas temperature in the reactor may be in the range of 250°C after 3 min of operation as shown in Fig. 8. On the other hand,  $\text{NO}_x$  and CO generations were as high as 65 ppm and 29 ppm, respectively which was not reflected during the desorption measurements.